Research Article 2017, **2**(1), 06-09 Advanced Materials Proceedings

Optical property and AC conductivity RF sputtered *N*-doped ZnO thin films

Trilok K. Pathak[1,2*], L. P. Purohit[2*]

[1]*Department of Physics, University of the Free State, Bloemfontein, 9301, South Africa*
[2]*Departments of Physics, Gurukul Kangri University, Haridwar, Uttarakhand 249404, India*

[*]Corresponding author, Tel: (+91) 01334-212198; Fax: (+91) 01334-246811; E-mail: tpathak01@gmail.com; lppurohit@gmail.com

Received: 30 March 2016, Revised: 19 September 2016 and Accepted: 30 November 2016

DOI: 10.5185/amp.2017/103
www.vbripress.com/amp

Abstract

ZnO and ZnO:N thin films were deposited on plane glass substrate using RF sputtering method. The crystalline structure and surface morphology of the film was investigated using XRD and SEM. The XRD patterns of ZnO thin films have largest crystalline orientation for the (002) peak and shows wurtzite structure. The ZnO thin films composed of dance packing, grains without any cracks indicating uniform grain size distribution. The transmittance and absorbance of ZnO thin film was measured using UV-VIS-IR spectrophotometer in the wavelength range 200 nm-800 nm. The band gap of ZnO film was 3.26 eV calculated by Tauc's plot method. Photoluminescence property was also investigated at the excitation wavelength 325 nm. A.C. conductivity measurements carried out on the ZnO/ZnO:N thin films at room temperature in the frequency range 10 KHz to 0. 1MHz. This measurement also helps to distinguish between localized and free band conduction. The study demonstrated that ZnO and ZnO:N thin films fabricated by RF sputtering method can be used in electronic and optoelectronic applications due to high transmittance in visible region, large bandgap and localized conduction.
Copyright © 2016 VBRI Press.

Keywords: RF sputtering, X-Ray diffraction, band gap, AC conductivity.

Introduction

Zinc oxide (ZnO) is a unique semiconductor material that exhibits numerous useful properties for applications in solar cells, optoelectronics, sensors and biomedical sciences [**1, 2**]. ZnO is a type II-VI semiconductor, has a large band gap (3.37 eV) and a high excitation binding energy (60 meV) [**3**]. ZnO with a wurtzite structure is naturally an *n*-type semiconductor because of a deviation from stoichiometry due to the presence of intrinsic defects such as O vacancies (V_O) and Zn interstitials (Zn_i) [**4**]. The *n*-type doping of ZnO is relatively easy compared to *p*-type doping. The *p*-type doping in ZnO may be possible by substituting either group-I elements (Li, Na, and K) for Zn sites or group-V elements (N, P, and As) for O sites. Among possible acceptor dopants, nitrogen is a good candidate for producing a shallow acceptor level in ZnO [**5**]. Lim et al. discussed about high performance thin film transistor on nitrogen doped ZnO thin films [**6**]. Xu et al. used NO as the dopant source to deposit p-type ZnO thin films [**7**]. But very few studies reported AC conductivity of ZnO and ZnO:N thin films. There are various techniques, which were used to synthesize N doped ZnO thin films such as chemical vapor deposition (CVD) [**8**], pulsed laser deposition (PLD) [**9**], molecular beam epitaxy (MBE) [**10,11**], metal organic chemical vapour deposition (MOCVD) [**12**], radio frequency (RF) magnetron sputtering [**13,14**] and the sol-gel technique [**15**]. Among these techniques RF magnetron sputtering is best technique to obtain p-type conductivity with high carrier concentration, mobility and good result of AC conductivity at high frequency [**16**].

In this paper, we deposit thin films using RF sputtering method and studied structural, optical and AC conductivity of ZnO and ZnO:N thin films. The effect of frequency on AC conductivity at different concentration of nitrogen also investigated. All the properties are investigated at room temperature.

Experimental

ZnO powder (Loba chemical, 99.99 % purity) was used to prepare the ZnO targets for the thin films produced by RF sputtering. An amount of 25 g of ZnO powder was taken in a disc and compressed up to a pressure of 10 ton by using a palletize machine. The prepared target was sintered at 450°C for 5 h. The sintered target was used for the deposition of the thin films by RF sputtering. A coating unit (planer magnetron sputtering unit modal: 12″ MSPT) was used. Argon (Ar) gas of high purity was used as sputtering gas. The ultrasonically cleaned glass substrates were used to the deposition in the sputtering

chamber. The sputtering chamber was first pump down from atmospheric pressure to a base pressure of 5×10^{-6} Torr, then Ar gas was introduced into the chamber. When the pressure of the chamber has reached ~5×10^{-2} Torr, the RF power supply was switched ON and the power was hold at 160 W for 30 min. The thin films were deposited on the glass substrates. The thickness of sputtered thin films was about 200 nm. Nitrogen (N_2) gas was supplied by mass flow controlled (MFC) inlets. N_2 was added with increased in the flow rates, with exhaust part adjusted to maintain constant chamber pressure. 3 SCCM N_2 and 5 SCCM N_2 doped thin films, N_2 gas was used in conjunction with Ar gas.

The deposited thin films by RF sputtering were used to investigate the structural, Optical and AC conductivity of ZnO/ZnO:N thin films. X-ray diffraction (X'pert Pro) was used to analyze crystalline structure of films and crystallite size. SEM (EVO-40 ZEISS) was used for the surface morphology. UV-VIS-IR spectrophotometer (Schimadzu-3600) was used for transmittance of thin films. The band gap of the sample was determined using Tauc's plot method. The PL data was recorded using F-4600 FL spectrophotometer. The AC conductivity was also using measured LCR meter. All measurements were carried out at room temperature.

Result and discussion

X-ray diffraction analysis

Fig. 1 shows the X-ray diffraction of undoped and N doped ZnO thin films deposited at room temperature on glass substrate with different N_2 concentration. It is evident that only (002) diffraction peak is indexed as the hexagonal wurtzite crystal structure of ZnO (JCPDS card no. 36-1451). Strong preferential growth is observed along (002) plane indicating that the films are oriented along c-axis [**17**].

As seen from figure, the diffraction angle of the (002) peaks shift towards small angle. The Crystallite size increases with N_2 concentration of these films as estimated by Scherer's formula (Equation 1) [**18**].

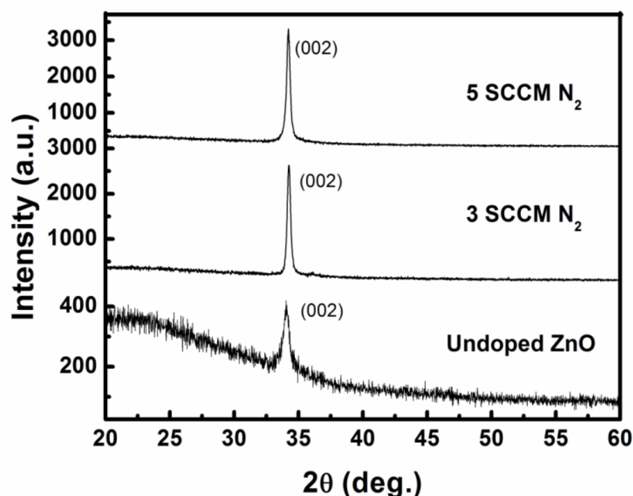

Fig. 1. XRD pattern of ZnO/ ZnO:N thin films.

$$D = \frac{K\lambda}{\beta \cos \theta} \quad (1)$$

where, K is the constant taken to be 0.94, λ is the wavelength of X-Ray used ($\lambda_{Cu\alpha}$ =1.54 Å) and β is full width half maxima (FWHM).

Table 1. Crystallite size and bandgap of ZnO/ZnO:N thin films.

Sample	Diffraction angle (2θ)	FWHM (degree)	Crystallite Size (nm)	Bandgap (eV)
Undoped ZnO	34.07	0.2856	29.09	3.26
3 SCCM N_2 ZnO	34.43	0.2448	33.97	3.18
5 SCCM N_2 ZnO	34.19	0.1632	50.92	3.25

The crystallite size increases with increase N_2 concentration from 29nm to 50 nm and the peak (002) shifted very little range may be due to generation of some strain.

Surface morphology studies

SEM image of undoped and N doped ZnO thin films are shown in **Fig. 2**. From micrograph, it is observed that there is growth of small square shape crystallites. The grain size increases continuously for undoped to doped ZnO samples. The grain size for 5 SCCM N_2 doped ZnO thin films was observed 52 nm which is correspond to the crystallite size which is measured by the XRD analysis. Xiao et al. [19] find the same SEM results when nitrogen doped ZnO thin films deposited by plasma enhanced chemical vapour deposition. The element analysis is also done by EDX for the sample 3 SCCM N_2. It is confirmed that the sample contains Zn, N in certain weight and atomic percentage.

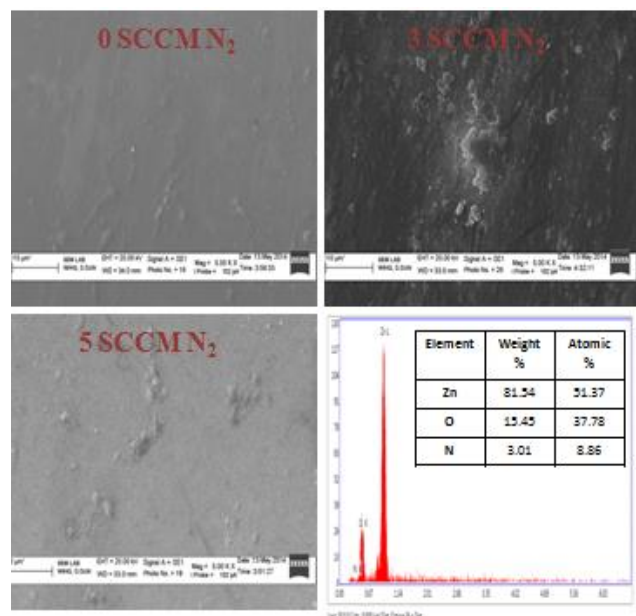

Fig. 2. SEM image and element analysis of N doped ZnO thin films.

Copyright © 2016 VBRI Press

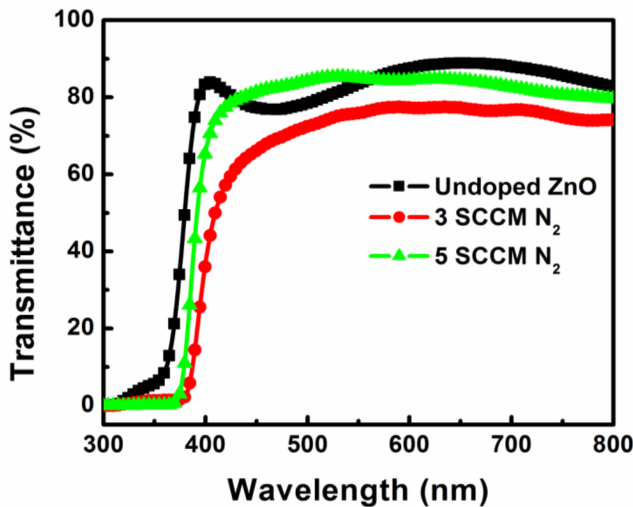

Fig. 3. Transmittance Spectra of undoped/ N doped ZnO thin films.

Optical studies

The wavelength dependent optical transmission spectra of undoped and N doped ZnO thin films deposited at different nitrogen concentration are shown in **Fig. 3**. The films show an average transmittance of about 80%, indicating that they are transparent in the visible region. The maximum transmittance is observed for undoped ZnO thin film and it decreases with doping concentration. The optical interference pattern in transmittance spectra shows good smooth thin films.

The optical energy band gap of the film was calculated from fundamental absorption edge of the films. For the allowed direct transition, the variation of α with photon energy (hυ) is obeys Tauc's plot method [**20**].

$$(\alpha h\nu)^2 = A(h\nu - E_g) \tag{2}$$

where, A is the constant for direct transitation, E_g is the energy gap, h is Plank's constant and ν is the frequency of incident radiation. The curve between $(\alpha h\nu)^2$ vs. hν is shown in **Fig. 4**.

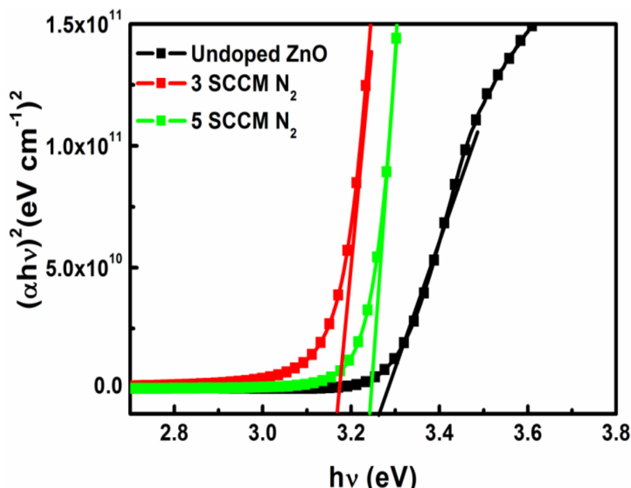

Fig. 4. Optical bandgap of undoped/ N doped ZnO thin films.

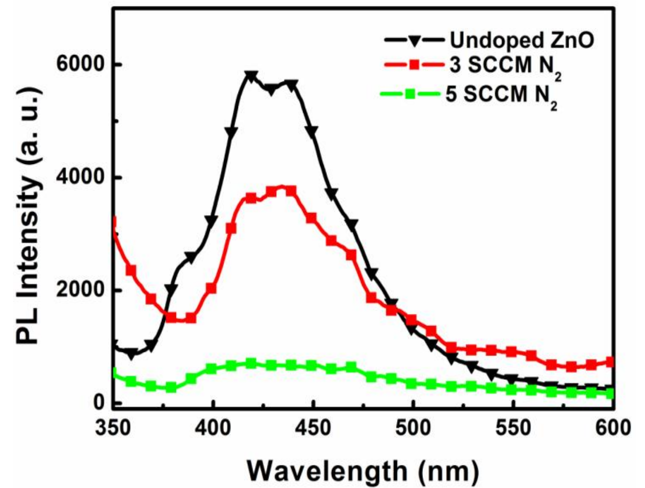

Fig. 5. PL results of undoped/ N doped ZnO thin films

The bandgap is maximum 3.26 eV for undoped ZnO as doping occur first the bandgap decreases to 3.18 eV as 3 SCCM N_2 and further increases if doping concentration of nitrogen increases. **Fig. 5** shows the PL spectra undoped/ N doped ZnO thin films. The broad emission band is observed ranging from 380 nm- 500 nm they are near-band-edge (NBE) ultraviolet emission. All the films exhibit a predominant NBE emission at around 3.2 eV. This indicates that all the films have high optical quality. Stavale et al. [**21**] find the similar PL results for N doped ZnO. He observed that 730 nm defect peak is revealed in addition to the band recombination peak at 373 nm.

The intensity of the defect peak increases when growing the film at reducing conditions or inserting nitrogen into the oxide lattice. The films have near ultraviolet PL peaks in agreement with the optical bandgap of the films. The peak wavelength becomes shorter with decreasing doping concentration and increasing nitrogen flow rate, while at the same time the PL intensity decreases. This factor can be use to designers of optoelectronics devices optimized for specialized applications.

AC conductivity

The AC transport properties, ac conductivity are an important parameter, used to characterize the dielectric properties of materials. Measurement of AC conductivity of semiconductors has been extensively used to understand the transport mechanism in these materials to investigate the nature of defect centers [22], since they play a major role in the conduction process. A.C. measurements provide information about the interior of the materials in the region of relatively low conductivity. This measurement also helps to distinguish between localized and free band conduction. In the case of localized conduction, the a.c. conductivity increases with frequency, while in the free band conduction the conductivity decreases with frequency. This increase in ac conductivity may relate to the interfacial polarization and electrical conduction. AC conductivity is calculated by using the relation,

Copyright © 2016 VBRI Press

S = t /R×a (3)

where *t* is the thickness, *a* the area of cross-section and *R* the bulk resistance of the sample.

It is seen that a.c. conductivity increases with the increase of frequency. The a.c. conductivity is found to depend on frequency as.

$$\sigma(\omega)=A\omega^{s} \quad (4)$$

where, exponent s is found to be temperature dependent and has a value s=1, A is a constant which independent of frequency and dependent on temperature and ω is angular frequency.

AC conductivity measurements carried out on the undoped/N doped ZnO thin films prepared by RF sputtering at room temperature in the frequency range (10 KHz to 0. 1MHz). **Fig. 6** shows the variation of a.c. conductivity for undoped and N doped ZnO thin films within frequency range 10 KHz to 0.1MHz. The conductivity exhibits a nearly frequency-independent behaviour at low frequency region and dispersion at higher frequency. The maximum conductivity of 2.4×10^{-6} S cm^{-1} was achieved for samples with 5 SCCM N_2 doped ZnO film thin film.

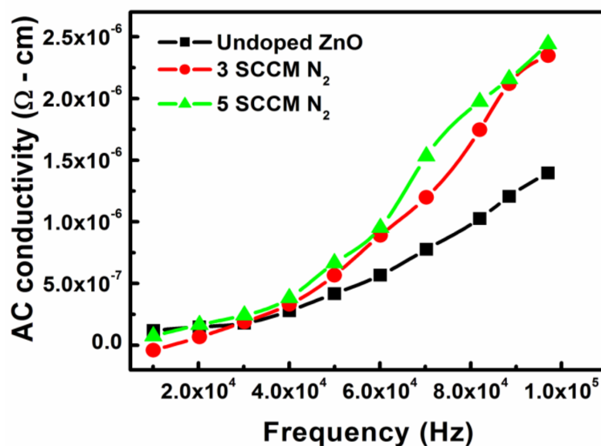

Fig. 6. AC conductivity of undoped/ N doped ZnO thin films.

Conclusion

ZnO and nitrogen doped ZnO thin films successfully synthesis on glass substrate using RF sputtering method. The single crystalline thin films are obtained corresponding to the peak (002) which satisfied the condition of hexagonal wurtzite structure. The crystallite size increases from 29 to 50 nm as nitrogen flow rates increased to 5 SCCM N_2. SEM results confirm the dense and smooth surface obtained for nitrogen doped ZnO thin films. The films are about 80 % transparent in the visible region. The bandgap varies in the range 3.18 to 3.26 eV with different flow rates of nitrogen. The big hump of PL peak of ZnO in obtained in the range 350-550 nm. In Nitrogen doped thin films AC conductivity increases with increasing frequency. This type of variation is indicative of localized conduction because in case of free band conduction a.c. conductivity decreases with increasing frequency.

Acknowledgement

The authors are thankful to Department of Science and Technology (DST), Govt. of India for providing facilities under FIST program. The authors are also thankful to Director, Wadia Institute of Himalayan Geology, Dehradun (India) for providing XRD and SEM facilities.

References

1. Dai, L. P.; Deng, H.; Mao, F. Y.; Jang, J. D.; *J. Mater. Sci: Mater Electron*, **2008**, *19*, 727.
2. Shekhar, A.; Tiwari, A.; Shukla, S. K.; Vamakshi, Minakshi, Anand; Advanced Materials Letters, 2012, 3, 421.
3. Karlsson, T.; Ross, A.; *Solar energy materials*, **1984**, 10, 105-119.
4. Jebril, S.; Kuhlmann, H.; Muller, S.; Ronning, C.; Kienle, L.; Duppel, V.; Mishra, Y. K.; Adelung, R.; *Crystal growth and design communication*, **2010,** *10*, 2842.
5. Kobayashi, A.; Sankey, O. G.; Dow, J. D.; *Phys. Rev. B*, **1983**, *28*, 946.
6. Lim, S. J.; Kwon, S. j.; Kim, H.; *Appl. Phys. Lett*., **2007**, *91*, 183517.
7. Xu, W.; Ye, Z.; Zhou, T.; Zhao, B.; Zhu, L.; Huang, J.; *Journal of Crystal Growth*, **2004**, *265*, 133.
8. Sen Chien, F.S.; Wang, C.R.; Chain, Y.L.; Wu, R.J.; *Sensor Actuat Phys. B*, **2010,** 144, 120.
9. Zhu, B.L.; Zhao, X.Z.; Su, F.H.; Wu, X.G.; *Vacuum*, **2010,** 84, 1280.
10. Opel, M.; Geprägs, S.; Althammer, M.; Brenninger, T.; Gross, R.; *J. Phys. D: Appl. Phys*., **2014,** *47*, 034002.
11. Heo, Y.W.; Ip, K.; Perton, S.J.; Norton, D.P., Budai, J.D.; *Applied Surface Science*, **2006,** *252*, 7442.
12. Mohanta, S.K.; Kim, D.C.; Cho, H.K.; Tripathy, S.; *J. Cryst. Growth*, **2008**, *310*, 3208.
13. Li, W.J.; Kong, C.Y.; Ruan, H.B.; Fang, L.; *Solid state Communications*, **2012,** *152*, 147.
14. Li, W.; Kong, C.; Qin, G.; Ruan, H.; Fang, L.; *Journal of Alloys and Compounds*, **2014**, *609*, 173.
15. Nian, H.; Hahn, S.H.; Koo, K.K.; Shin, E.W.; Kim, E.J.; *Materials Letters*, **2009,** *63*, 2246.
16. Balakrishnan, L.; Gowrishankar, S.; Premchander, P.; Gopalakrihnan, N.; *Journal of Alloys and Compounds*, **2012,** *512*, 235.
17. Chen, K. J.; Hung, F. Y.; Chang S. J.; Young, S. J.; *Journal of Alloys and Compounds*, **2009**, *2*, 674.
18. Khan, Z. R.; Zulfequar, M.; Khan, M. S.; *Materials Science and Engineering B*, **2010**, *3*, 145.
19. Xiao, Zhiyan; Liu, Yichun; Zhang, Jiying; Zhao, Dongxu; Lu, Youming; Shen, Dezhen; Fan, Xiwu; *Semiconductor Science and Technology*, **2005**, *8*, 796.
20. Pathak, T. K.; Kumar, V.; Swart, H.C.; Purohit, L.P.; Physica E, **2016,** *77*, 1.
21. Stavale, F.; Pascua, L.; Nilius, N.; Freund, H. J.; *J. Phys. Chem. C*, **2014**, *118*, 13693.
22. Tewari, S.; Bhattacharjee, A.; Sahay, P.P.; *J. Mater. Sci.,* **2009**, *2*, 534.

Copyright © 2016 VBRI Press